Available online at www.sciencedirect.com

ScienceDirect

Biochimica et Biophysica Acta 1778 (2008) 1259–1266

Biochimica et Biophysica Acta BBA

www.elsevier.com/locate/bbamem

Lysophosphatidylcholine–arbutin complexes form bilayer-like structures

M. A. Frías [a], B. Winik [b], M. B. Franzoni [c], P. R. Levstein [c], A. Nicastro [d,e], A. M. Gennaro [d,e], S. B. Diaz [a], E. A. Disalvo [f,*]

[a] *Instituto de Química Física, Facultad de Bioquímica, Química y Farmacia, Universidad Nacional de Tucumán, San Lorenzo 456 (4000) Tucumán, Argentina*
[b] *Laboratorio de Microscopía Electrónica, Universidad Nacional de Tucumán, LAMENOA Argentina*
[c] *LANAIS de RMN, Facultad de Matemática, Astronomía y Física, Universidad Nacional de Córdoba, Argentina*
[d] *Departamento de Física, Facultad de Bioquímica y Ciencias Biológicas, Universidad Nacional del Litoral (UNL), Paraje El Pozo S/N (3000) Santa Fe, Argentina*
[e] *INTEC (CONICET-UNL), Güemes 3450 (3000) Santa Fe, Argentina*
[f] *Laboratorio de Fisicoquímica de Membranas Lipídicas, Facultad de Farmacia y Bioquímica, U. B. A. Junín 956 2°P (1113) Buenos Aires, Argentina*

Received 5 September 2007; received in revised form 13 January 2008; accepted 4 February 2008
Available online 14 February 2008

Abstract

Arbutin is known to suppress melanin production in murine B16 melanoma cells and inhibit phospholipase action. This encourages the possibility to stabilize it in lipid aggregates for its administration in medical applications. Thus, it was of interest to demonstrate that monomyristoylphosphatidylcholine (14:0 lysoPC) and arbutin may form association complexes. This was studied by Electron Microscopy (EM), ^{31}P Nuclear Magnetic Resonance (^{31}P NMR), Electronic Paramagnetic Resonance (EPR) and Fourier Transform Infrared Spectroscopy (FTIR). EM images show the formation of particles of c.a. 6 nm in diameter. For a 1:1 lysoPC–arbutin molar ratio ^{31}P NMR shows a spectrum with a shoulder that resembles the axially symmetric spectrum characteristic of vesicles. The addition of La^{3+} ions to the arbutin–lysoPC complex allows one to distinguish two phosphorous populations. These results suggest that arbutin–lysoPC forms vesicles with bilayers stabilized in an interdigitated array. FTIR spectroscopy shows that arbutin interacts with the hydrated population of the carbonyl groups and with the phosphates through the formation of hydrogen bonds. It is interpreted that hydrophobic interactions among the phenol group of arbutin and the acyl chain of lysoPC are responsible for the decrease in acyl chain mobility observed at the 5th C level by EPR. A model proposing the formation of interdigitated bilayers of arbutin-lysoPC could explain the experimental results.

Keywords: LysoPC; Arbutin; Interdigitation; FTIR interactions; ^{31}P NMR; Electron Microscopy; Electron Paramagnetic Resonance

1. Introduction

Arbutin is a well known natural product that appears in plants under hydric stress. Because of that it has been used as an additive to preserve cell membrane structure in freeze thaw processes. In addition, it is an inhibitor of phospholipase A_2 and tyrosinase [1,2]. The mechanism of these effects is not completely understood.

As one of the products of the phospholipase A_2 is lysoPC and our previous results show that arbutin avoid the lysis produced by lysoPC on liposomes with defects [3,4], it was of interest to study the possible interaction between lysoPC and arbutin in order to explain a possible mechanism of membrane stabilization, i. e. the hypothesis is that lysoPC and arbutin may accumulate in bilayers forming more bilayers.

In addition, arbutin is known to suppress melanin production in murine B16 melanoma cells. This encourages the possibility to stabilize it in lipid aggregates for its administration in medical applications [5].

For this it was of interest to demonstrate the possibility that lysoPC and arbutin may form association complexes.

According to the phase diagram lyso phosphatidylcholines, in their pure form, stabilize as micelles in aqueous phases at 25 °C due to their conical shapes in which the area of the hydrated head group is larger than that swept by the single hydrocarbon chain [6,7]. The effects of lysoPC have been studied in a number of systems. It has been shown that it produces the lysis of red blood

* Corresponding author. Fax: +54 11 45083645.
E-mail address: eadisal@yahoo.com.ar (E.A. Disalvo).

0005-2736/$ - see front matter © 2008 Elsevier B.V. All rights reserved.
doi:10.1016/j.bbamem.2008.02.002

cells and of PC bilayers at the transition temperature producing the disruption of the bilayer into mixed micelles [8]. Also, upon cooling a micellar solution of 1-palmitoyllysophosphatidylcholine below the chain-melting temperature a transition to a lamellar, most likely interdigitating organization has been reported [6].

Further studies have shown that the effect of lysoPC on DMPC bilayers can be related to the presence of defects at the membrane surface due to the coexistence of gel and fluid phases [9]. In addition, it was also shown that lysoPC inserts into defects in the P_β phase [10].

LysoPC interacts with the carbonyl groups when inserting in lipid membranes of DMPC. Interestingly, polyhydroxilated compounds concerting H-bonds with these groups are able to counterbalance the lytic effects of lysoPC on the P_β phase [11]. In these cases, arbutin, a phenol glucopyranoside is able to inhibit the lysoPC detergent effect in DMPC liposomes at 18 °C [4].

In those studies, the lytic effect was followed by changes in the light scattering of DMPC–arbutin liposome dispersions. It was observed that previous to the disruption of the liposomes, an increase in the light scattering was apparent. This effect was similar to that observed when lysoPC was added to DMPC–cholesterol bilayers. This was explained by the stabilization of the bilayer conformation due to the accumulation of lysoPC in the PC bilayer containing arbutin. Only when an excess of arbutin–lysoPC was attained above the maximum of turbidity, the lysoPC disrupted the bilayer to form micelles.

As lysoPC is produced "in situ" by phospholipase hydrolysis and arbutin is an inhibitor of this enzymatic action, it may be plausible that lysoPC–arbutin interaction may counteract the lytic activity of this enzyme in PC bilayers.

In this regard, it is well known that the mixing of lysoPC with cholesterol or with phosphatidic acid can form bilayers [12]. Thus, a possible explanation to the increase in turbidity could be the formation of lysoPC–arbutin association complexes.

With this base, we have studied the properties of lysoPC–arbutin mixtures in order to define the formation, shape, structure and properties of the aggregates.

2. Materials and methods

2.1. Lipids and chemicals

Mono myristoyl phosphatidylcholine (LysoPC), was obtained from Avanti Polar Lipids, Inc (Alabaster, AL) and arbutin (4-hidroxyphenyl-β-D-glucopiranoside) and D_2O from Sigma-Aldrich (Saint Louis, MO). The purity of the lipid and of the arbutin was checked by running the FTIR spectra of lyophilized samples and by differential scanning calorimetry (DSC). All other chemicals were of analytical grade, and water tridistilled.

2.2. Light scattering measurements

LysoPC stock solutions of a concentration 1.14 mM were prepared in tridistilled water.

The turbidity changes at 25 °C were followed by measuring the changes in the absorbance at 450 nm in a Beckman DU 7500 spectrometer by adding known amounts of the stock lysoPC solution to a measured volume of water or 10 mM arbutin solution. In a parallel assay, a 2 ml solution of lysoPC above the critical micellar concentration was titrated with known volumes of 10 mM arbutin solution or of water.

2.3. Transmission electron microscopy

The samples of different arb/lysoPC ratios were primary fixed in Karnovsky fixative buffered with 0.1 M phosphate, pH 7.4 plus 1 mM calcium chloride. After 3 h at 4 °C, pellets were washed in the same buffer and transferred to 1% osmium tetroxide overnight. Samples were then rinsed in distilled water and treated with an aqueous solution of 2% uranyl acetate for 40 min. After fixation, samples were gradually dehydrated in a series of alcohols of increasing strength, followed by acetone [13]. The infiltration with the embedding medium was performed in Spurr resin (Pelco Int., CA, U.S.A).

Ultrathin sections mounted on copper grids were stained with uranyl acetate and lead citrate and examined with a Zeiss EM 109 transmission electron microscope with a resolution of 0.3 nm.

To avoid artifacts, ten samples for each condition (lysoPC alone and lysoPC plus arbutin) were processed in the same condition. $CaCl_2$ was added as recommended to prevent the loose of lipids during dehydration and fixation of samples.

2.4. Electron paramagnetic resonance (EPR) measurements

The liposoluble spin label 1-Palmitoyl-2-Stearoyl (5-Doxyl)-*s*, *n*-Glycero-3-Phosphocholine (5 PCSL, Avanti Polar Lipids, Alabaster, USA), was incorporated to the lysoPC in chloroform solution. The spin label/lysoPC molar ratio was less than 1%, in order to avoid line broadening effects in the EPR spectra. After evaporating the organic solvent under nitrogen stream, the samples were kept in vacuum overnight and subsequently hydrated at 25 °C with Tris buffer, pH 7.4, or with arbutin solutions in Tris buffer, pH 7.4, to a final lysoPC concentration of 25 mM. Arbutin was present in three different concentrations: 375 mM, 37.5 mM and 3.75 mM to achieve the lysoPC–arbutin ratios of 1:15, 1: 1.5, and 1:0.15.

Aliquots of the labeled lipid dispersions (usually 20 μl) were transferred into glass capillaries (1-mm i. d.), which were flame sealed and placed into 4-mm quartz tubes. The EPR spectra were recorded at fixed temperatures (25 °C) at 9.8 GHz (X Band) in an ER-200 spectrometer (Bruker Analytische Messtechnik GMbH, Karlsruhe, Germany). Temperature was controlled with a Bruker ER 4111VT unit. Field modulation frequency was 100 kHz, and microwave power was fixed at 3 mW.

The outer hyperfine splitting $2A_{max}$ was obtained from each spectrum. This parameter can be used to characterize the rotational disorder and rotational rates of the spin labeled lipid chain segment, and it is a useful indicator to compare segmental mobility in a series of similar samples [14]. The possible values of $2A_{max}$ range between the isotropic limit of about 32 G, expected for a spin label performing unrestricted fast reorientation in an isotropic (completely disordered) environment, and the rigid limit value of about 64 G corresponding to an immobilized spin label in a rigid acyl chain environment [15–17].

2.5. ^{31}P nuclear magnetic resonance

A Bruker Avance II spectrometer was used (^{31}P NMR frequency ν_0= 121.4958 MHz).

For all the experiments we applied the Waltz decoupling sequence for the ^1H nuclei. The Pi/2 pulse for ^{31}P was 5.4 μs.

The spectra of lysoPC and lysoPC with arbutin were compared in the same conditions with that of a lipid known to form lamellar structures in order to dilucidate the possible presence of bilayers. As it is known, micelles and small vesicles give an isotropic signal, whereas, lamellar structures such as liposomes give a shoulder at lower field [6,21,27]. In addition, La^{3+} was added to lysoPC and lysoPC plus arbutin suspensions in order to suppress the signal of the exposed phosphate groups. In the case of micelles, as all the phosphates are facing the water phase, the signal is completely suppressed. In the case of small vesicles, the isotropic signal should persist because the phosphates towards the inner lumen are not affected by the presence of La^{3+} in the suspending solution. The area under the peak of lysoPC plus arbutin without La^{3+} and that under the peak of the same suspension with La^{3+} allow calculating the ratio of phosphate groups exposed to La^{3+} and those protected from its action.

2.6. FTIR measurements

FTIR Perkin Elmer GX spectrophotometer, provided with a DTGS detector, was used. The resolution of the equipment employed was 1 cm^{-1}. To study the

interaction of arbutin with the phospholipid head groups, lipids were dispersed in D_2O and H_2O using a cell with AgCl windows at 25 °C. A total of 30 scans were done in each condition and the spectra were analyzed using the mathematical software GRAMS. The deconvolution algorithm was applied to define the contours of overlapping bands. The bands in the mixtures were assigned to the carbonyl and phosphate groups by comparison with pure lipids dispersed in D_2O and H_2O, respectively.

Mean values of the main bands in each condition were obtained from a total of three different batches of samples.

The components of the C=O stretching bands, were obtained by Fourier Self Deconvolution. The mathematical software GRAMS/32 Spectral Notebase was used to obtain the peak frequencies of the component bands reported for the two populations of carbonyl groups one centered at 1725.5 cm^{-1} and another at 1715.5 cm^{-1} [18–20].

3. Results

The increase in turbidity observed by the addition of lysoPC to a solution of 10 mM arbutin is much higher than that corresponding to the formation of lysoPC micelles in pure water at a critical micellar concentration (cmc) of 0.03–0.04 mM. As deduced from Fig. 1A, the turbidity increase in the presence of arbutin is produced at much lower concentrations than the critical micellar concentration of lysoPC in water (see expanded insert). A first plateau is found for a 1:20 lysoPC–arbutin ratio and the second to a 1:1 lysoPC–arbutin. The addition of water to a suspension of 1.14 mM lysoPC, in which the lysoPC micelles are preformed, decreases the turbidity (data not shown). However, the titration with arbutin shows a similar turbidity increase as that observed in Fig. 1A (Fig. 1B). As a control, the addition of arbutin to water promotes a slight increase probably due to changes in the refractive index of the solution.

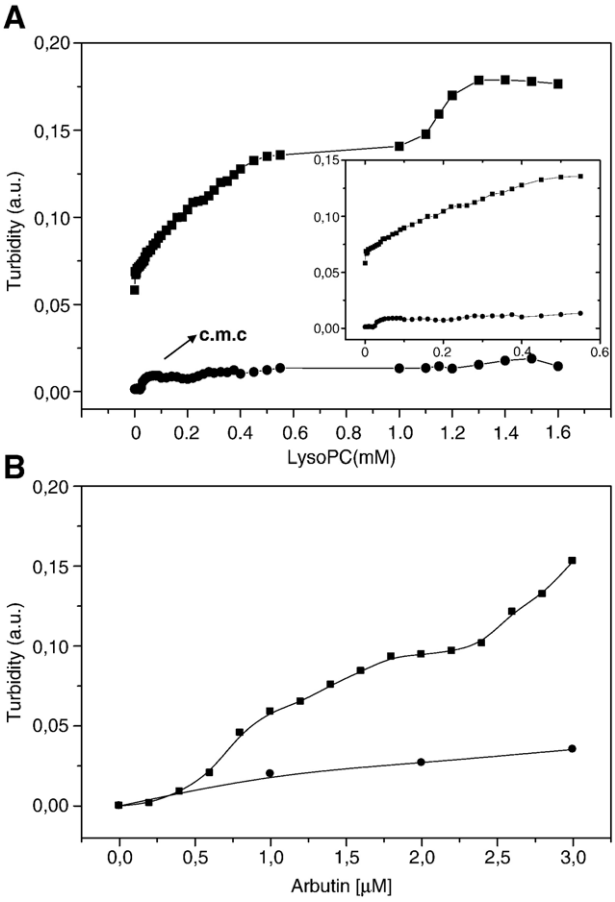

Fig. 1. Turbidity changes in mixtures arbutin–lysoPC. A. - Addition of 1.14 mM lysoPC aliquots to water (●) and to a 10 mM arbutin solution (■). Arrow indicates the critical micellar concentration of lyso (14:0) PC in water, at 25 °C. Insert: Turbidity increase at low concentrations of lysoPC. B. - Addition of volumes of water (●) or a 10 mM arbutin solution (■) to a suspension of 1.14 mM lysoPC.

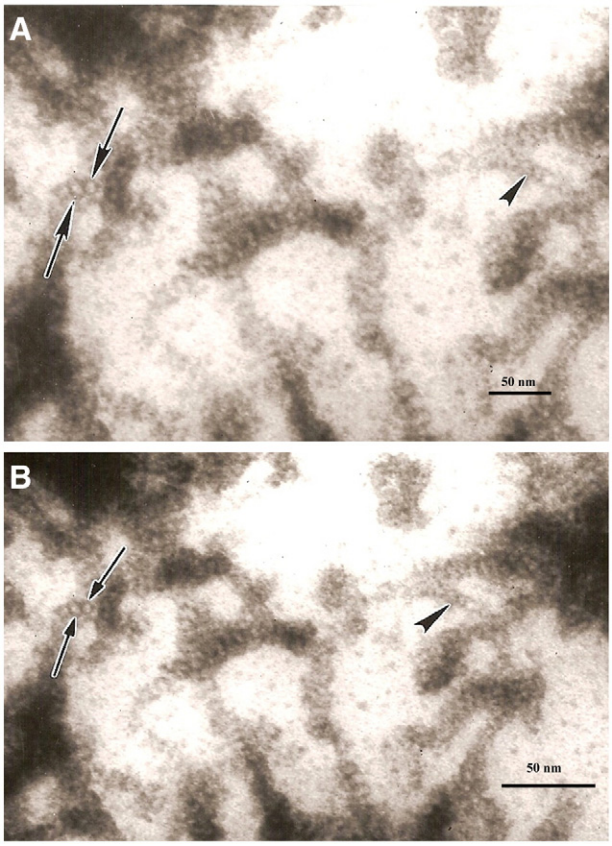

Fig. 2. Transmission electron microscopy images of the aggregates formed in an arbutin–lysoPC mixture (mol:mol ratio). A.- Note vesicles lined by electron-dense membrane (arrows). Arrow head/s indicates/s the clustering of vesicles in aggregates (×440.000). (Scale bar: 50 nm). B- ×300.500. (Scale bar: 50 nm). High magnification shows vesicles (arrows) and the aggregate of vesicle (arrow head).

Samples of the solution in Fig. 1B before adding arbutin or at a concentration corresponding to the plateau at the highest turbidity obtained were inspected by transmission electron microscopy. In the first case, no vesicles were observed. Instead, the examination of ultrathin sections of the lysoPC–arbutin mixtures with a transmission electron microscopy revealed small quasi spherical vesicles of a mean external diameter of about 6 nm and about 3.5 nm of internal diameter. Each vesicle is surrounded by an electron-dense envelope, while the lumen is electron-lucid without showing an internal structure (Fig. 2). The samples also showed a sequential clustering of the vesicles.

In conditions in which no vesicles were observed by EM, (pure lysoPC), the ^{31}P NMR showed a signal corresponding to micelles. In Fig. 3A, the signals corresponding to lysoPC

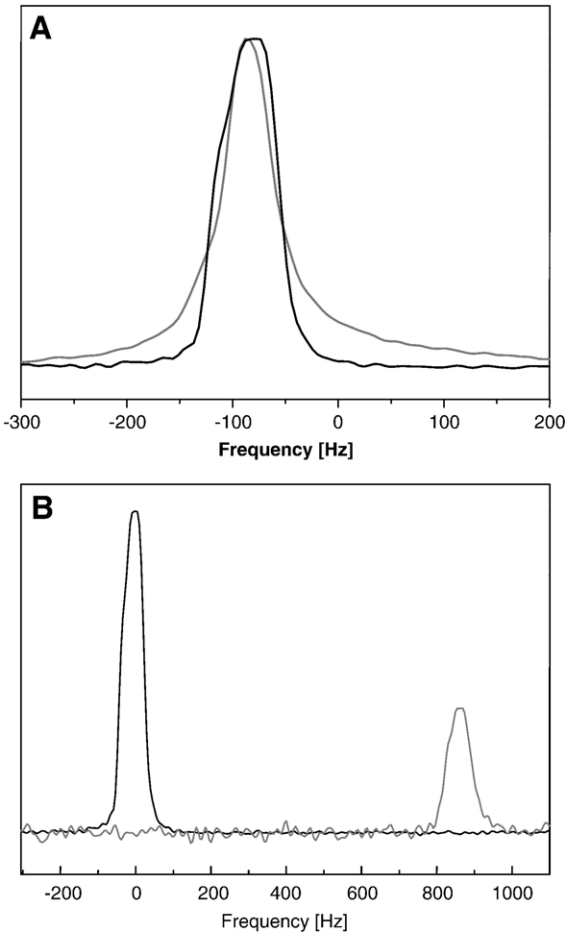

Fig. 3. ^{31}P-nmr signal of lysoPC and arbutin–lysoPC mixtures. A. LysoPC (—) and arbutin–lysoPC (▬) suspension. The full width at half height (FWHH) of the pure LysoPC is 53 Hz, while the FWHH of arbutin–LysoPC is 65 Hz. Notice the shoulder in the arbutin–lysoPC ^{31}P NMR spectrum. B. LysoPC–arbutin signal without (—) and with the addition of La^{3+}(▬) to the media.

micelles and that corresponding to the mixture lysoPC and arbutin obtained by ^{31}P NMR measurements are superposed. Lysophosphatidylcholine (lysoPC) micelles in water give rise to a narrow, isotropic phosphorus-^{31} NMR signal (approx. 0.5 ppm) as that reported either for micelles or small vesicles [5,20].

While the ^{31}P NMR linewidths of the pure lysoPC and lysoPC–arbutin samples are quite similar, 56 Hz and 65 Hz respectively, the signal of the mixture lysoPC–arbutin is not isotropic. This suggests the presence of larger aggregates in which the interactions between the magnetic dipoles are not completely averaged out (Fig. 3A). As known, typical asymmetric signals with a shoulder at lower fields are obtained in aqueous suspensions of phosphatidylcholines, which is usually ascribed to the formation of multilamellar aggregates [21]. In the lysoPC–arbutin mixture, the shoulder is slightly pronounced. However, it cannot be disregarded that large aggregates may coexist with small vesicles both formed by bilayers as shown in the microscopy images.

Upon addition of paramagnetic ions, the phosphorus signals are shifted downfield [21] (Fig. 3B). La^{3+} quenches the ^{31}P signal corresponding to all the phosphates exposed to the aqueous phase. The addition of La^{3+} to a lysoPC suspension results in a complete suppression of the signal. However, when La^{3+} is added to a mixture of lysoPC–arbutin a signal remains although displaced to lower values in ppm due to the extra field induced by the La^{3+}. This signal preserves the asymmetry.

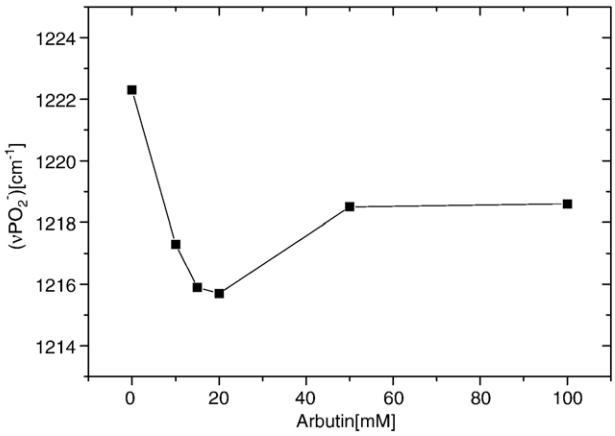

Fig. 4. Effect of increasing concentrations of arbutin on the antisymmmetric stretching band of phosphate groups of lysoPC.

This indicates that part of the population of phosphates are protected or isolated from the presence of La^{3+}. The ratio between inner and outer phospholipids obtained from the integration of the signals with and without La^{3+} is 47% protected–53% exposed. It should be emphasized that "inner" means not exposed to La^{3+}. It can occur that due to cluster formation, some phosphate groups, "external" from the point of view of the small vesicular structures are counted as "inner groups". This is why we prefer to label the two populations of phosphorus as protected or exposed.

In Fig. 4, the antisymmetric stretching phosphate band is shown to displace to lower frequencies, to reach a minimum at 20 mM arbutin for the lysoPC concentration used. At higher

Table 1
Effect of arbutin on the stretching band of the non hydrated (P_1) and hydrated (P_2) populations of carbonyl groups of lysoPC

Arbutin/ mM	$\tilde{\nu}_p$/cm^{-1} st C=O (P_1)	Standard deviation	$\Delta\tilde{\nu}$/ cm^{-1}	$\tilde{\nu}_p$/cm^{-1} st C=O (P_2)	Standard deviation	$\Delta\tilde{\nu}$/ cm^{-1}
0	1725.5	0.1	0.0	1715.5	0.1	0.0
10	1724.2	0.3	−1.3	1711.2	0.1	−4.3
15	1725.4	0.6	−0.1	1712.4	0.9	−3.1
20	1725.4	0.8	−0.1	1713.1	0.4	−2.4
50	1725.8	0.7	0.3	1712.1	0.3	−3.4
100	1725.9	0.5	0.4	1712.0	0.1	−3.5

Table 2
Effect of lysoPC on the aromatic double bond of arbutin

System	$\tilde{\nu}_p$/cm^{-1} St Antisym PO_2^-	$\Delta\tilde{\nu}$/cm^{-1}
C=C $_{arom}$ Solid arbutin	1512.7±0.3	0.0
C=C $_{arom}$ Arbutin 10 mM in D_2O	1509.7±0.8	−3.0
C=C $_{arom}$ Arbutin 10 mM with LysoPC	1511.2±0.4	−1.5

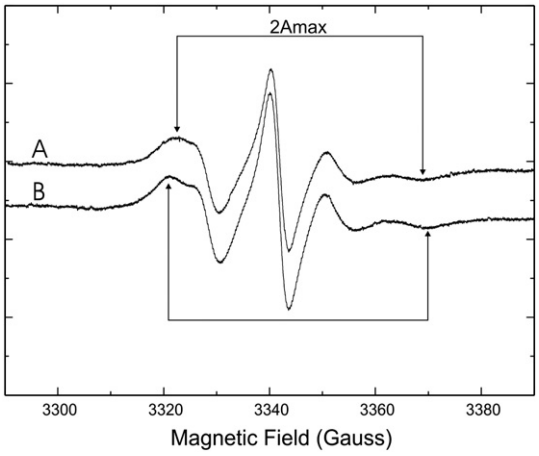

Fig. 5. Mobility of the acyl chains in the presence of arbutin as determined by EPR. EPR spectra of the spin label 5-PCSL in (A) lysoPC, and (B) lysoPC with arbutin. The concentrations are 25 mmol/l for lysoPC and 375 mmol/l for Arbutin.

concentrations, it increases and stabilizes above 50 mM. The symmetric stretching band is not affected.

In Table 1, the frequency of the FTIR bands corresponding to the CO groups for lysoPC in the presence and the absence of arbutin are shown. It is observed that the increase of arbutin concentration displaces the lower frequency band (corresponding to the hydrated population) to lower values with concentration, suggesting the formation of stronger H-bonds between C=O and arbutin than with water. In contrast, no effect on the non-hydrated population (the population giving a band at higher frequency without arbutin) is observed within the experimental error.

Another evidence of the association is provided by the bands of the aromatic double bonds of the phenol moiety of arbutin in the presence of lysoPC (Table 2). The frequency decreases when solid arbutin is dissolved in water, but recovers the values obtained in solid state in the presence of lysoPC.

The association of arbutin to lysoPC increases the acyl chain rigidity as shown using 5 PCSL as a probe. EPR experiments showed that the addition of arbutin to lysoPC increases acyl chain rigidity in comparison to pure lysoPC micelles (Fig. 5). The increase in the $2A_{max}$ hyperfine parameter (pointed by the arrows) indicates a restriction of the mobility of the acyl chains in the presence of arbutin. In Table 3, $2A_{max}$ values in lysoPC–arbutin aggregates are compared with those corresponding to DMPC bilayers at the gel and the liquid crystalline state.

This acyl chain stiffening in lysoPC–arbutin mixtures detected by EPR is congruent with the variation of CH_3 symmetric band in FTIR, which is displaced to lower frequencies with arbutin (Table 4). The decrease in the frequency is related to the increase of the van der Waals contact between the acyl chains [22].

Table 3
$2A_{max}$ values in the lysoPC–arbutin aggregates and DMPC bilayers at the gel and the liquid crystalline state

DMPC liquid crystalline (26 °C)	DMPC gel (20 °C)	LysoPC (26 °C)	LysoPC/arbutin (26 °C)
52.1 G	60.7 G	46.3 G	48.6 G

Table 4
Effect of Arbutin on the antisym and sym stretching bands of the CH_3 groups of lysoPC

Arbutin/ mM	$\tilde{\nu}_p$/cm^{-1} St Antisym CH_3	Standard deviation	$\Delta\tilde{\nu}$/ cm^{-1}	$\tilde{\nu}_p$/cm^{-1} St Sym CH_3	Standard deviation	$\Delta\tilde{\nu}$/ cm^{-1}
0	2955.5	0.1	0.0	2872.8	0.3	0.0
10	2956.5	0.4	0.9	2871.4	1.3	−1.3
15	2955.8	0.3	0.3	2870.6	0.1	−2.3
20	2956.3	0.3	0.8	2870.5	0.2	−2.3
50	2956.2	0.4	0.7	2870.6	0.1	−2.1
100	2956.5	0.2	1.0	2869.7	0.3	−3.1

4. Discussion

The clusters of vesicles observed by EM at ultra-structural level are consistent with the results obtained by ^{31}P-NMR indicating that part of the phosphates in the aggregates are faced towards the inner lumen and others to the outer media. The average vesicle size observed in Fig. 2 is around 6 nm for the external diameter and 3.5 nm for the internal one. In consequence, the thickness of the borderline should be around c.a. 1.25 nm, much thinner than for a bilayer in which the lipids are opposed tail to tail.

To achieve this thickness the membrane surrounding each vesicle can be understood considering that lipids in the presence of arbutin stabilize in an interdigitated array as that described in Fig. 6B.

The interaction of the lysoPC with arbutin results in a more rigid structure than that formed by micelles of pure lysoPC, as denoted by the increase in the $2A_{max}$ parameter in the EPR signal (Table 3). The effect of arbutin on the mobility of the acyl chains in lysoPC is in the same direction than that corresponding to DMPC bilayers from the fluid to the gel state although much lower in magnitude. This is congruent with the fact that micelles are structures in which the lipids are less packed due to the curvature [6].

The interaction of arbutin at several levels of the lysoPC molecule is put into relevance by the FTIR results. In contrast to what was observed in DMPC, arbutin affects the hydrated population of the carbonyl groups of lysoPC molecules, being the non hydrated population not affected. This suggests that, in the presence of arbutin, one carbonyl population remains facing the non polar interior and the other bound to the arbutin.

Thus, arbutin binding to the lysoPC appears weaker than to DMPC in which it binds to the non hydrated population forcing the hydrated one to dehydrate [4].

In addition, the increase in arbutin concentration up to 20 mM decreases the frequency of the antisymmetric stretching band of the phosphate groups. This suggests a hydrogen bonding interaction by the intercalation of arbutin. However, at larger concentrations, the frequency differences return to the values of the lipid without arbutin, reaching a constant value

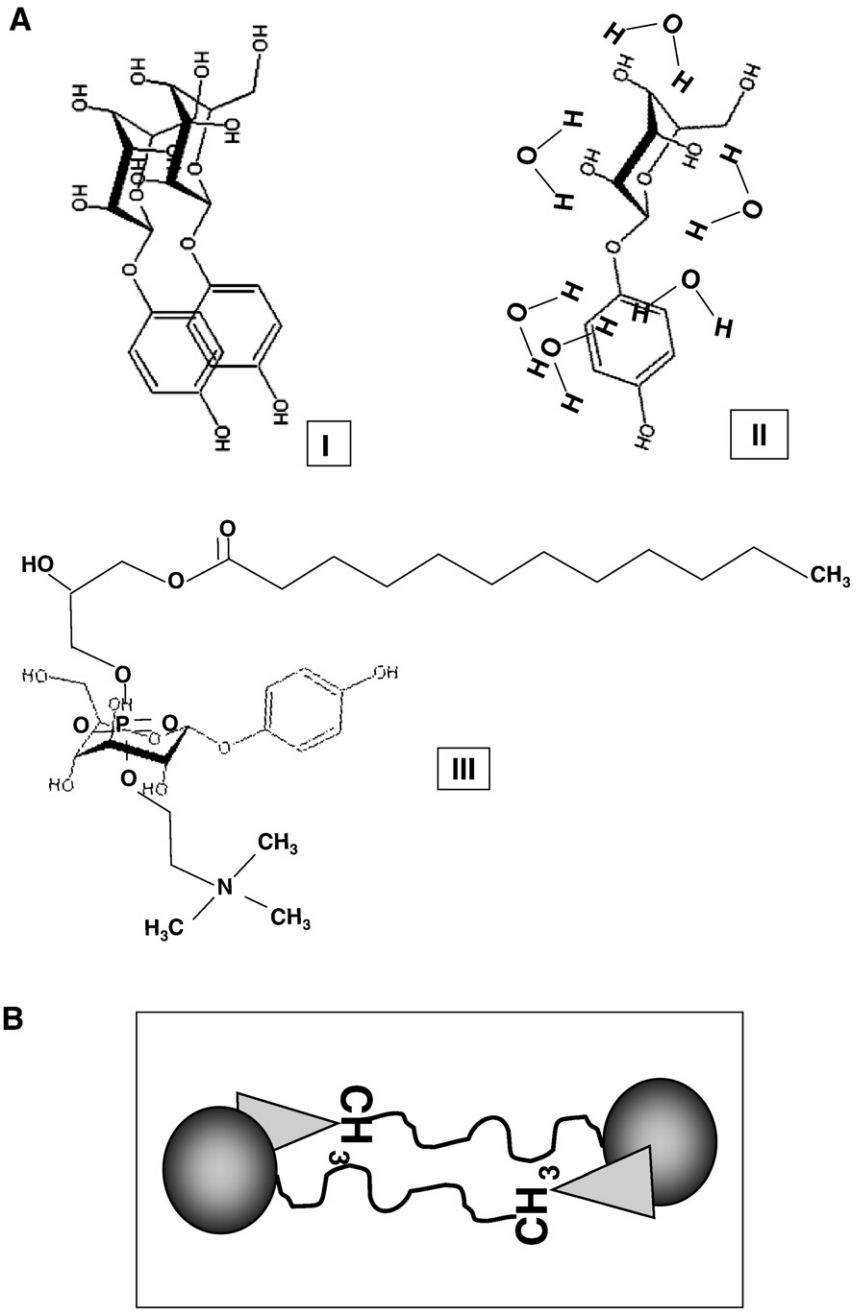

Fig. 6. Interaction of the phenol moiety with the CH_3 methyl group in lysoPC–arbutin interdigitated complex. A) Arbutin in solid (I), arbutin in the presence of water (II), and arbutin in the presence of lysoPC (III). B) Interdigitated stabilization of the lysoPC–arbutin complex.

above 50 mM. A similar trend is observed in the low frequency band of the carbonyl groups (Table 1).

The fact that the frequency difference does not decrease further above 20 mM would denote that even in the excess of arbutin no further association complexes are formed. If the frequency would have reached a constant value, it would imply that the excess of arbutin does not affect the former vesicles. However, the increase of frequency in the direction of the lysoPC without arbutin suggests that the bonds previously formed by arbutin with the lysoPC groups become weaker. This can be intepreted as a consequence of a subsequent process of aggregation.

Possibly after they are formed, an adhesion of the vesicles would take place congruent with the second plateau of Fig. 1A. This can be supported by the EM images in which the vesicles appear forming clusters. This aggregation may explain also the presence of phosphate groups that cannot be reached by La^{3+} in the ^{31}P NMR experiments of Fig. 3. The remaining signal could be ascribed to phosphates in the contacts of the particle surfaces. This effect could also be explained if the particles formed are micelles. However, the electron microscopy images show a dark borderline separating two electron-lucid media without showing an internal structure. This favors the idea of aggregated vesicles.

If this is the case, the possibility that the dark borderline correspond to a bimolecular membrane must be discussed. As shown, arbutin interacts with the lysoPC molecule by the binding to the P=O and the hydrated population of carbonyl groups. This picture is similar to that occurring with several sugars such as sucrose and trehalose, both of them having in common the glucose moiety, and all of them decreasing the P=O frequency by displacing water [23–25].

However, lysoPC also affects the phenol moiety of arbutin (Table 2). The frequency of the C=C aromatic double bond of arbutin shifts to values corresponding to the solid when lysoPC is present in the aqueous solution. In accordance, the terminal CH_3 group's symmetric frequency shift to lower values. This effect can be explained considering that lysoPC forms a complex with arbutin as is schematically described in Fig. 6A.

When arbutin is in the solid state (Fig. 6A, I), the ring–ring interactions are weak and therefore, the strength on the C=C, visualized as a high frequency value, is not affected. When arbutin is in water, the aromatic ring is able to form hydrogen bonds with the HO of water, displacing the C=C frequency to lower values (Fig. 6A, II). With the addition of lysoPC, the frequency increases towards the values in solid, denoting that the hydrogen bonding with water is displaced (Fig. 6A, III). This can be explained as a consequence of the hydrophobic interaction of the ring with the acyl chain, enhancing the van der Waals interactions. The increase in the van der Waals interactions gives place to a more rigid structure as inferred from the $2A_{max}$ values (Table 3). This behavior is similar to that found in DMPC bilayers when going from fluid to gel state [4].

In accordance, the CH_3 symmetric stretching band displaces to lower frequency values indicating a weakening of the CH bond strength (Table 4). This is congruent with the increase in the van der Waals interaction with the phenol groups as a consequence of the hydrophobic interaction. The acyl chain ends interact with the phenol ring in an interdigitated array as proposed in Fig. 6B [26].

The interdigitated layer formed by the terminal CH_3 of lysoPC and the phenol group of arbutin implies, in comparison to normal bilayer array, a decrease in the thickness. The 1.25 nm thickness of the dark dense borderline derived from the EM images would be compensated by an increase in the area, at constant volume. Considering that the area in the internal face (A_{int}) and the external face (A_{ext}) are 38.5 nm^2 and 113.04 nm^2, respectively, as derived from the EM images, the relation

$$A_{int}/A_{ext} = \left(\text{area}_{\text{lip inside}}/\text{area}_{\text{lip outside}}\right) \times (N^{\circ}\ \text{lipids inside}/N^{\circ}\ \text{lipids outside}) = 0.38$$

As the ratio between the inner and outer lipids (N° lipids inside/N° lipids outside) calculated from the ^{31}P NMR in the presence of La^{3+} is 47%/53%=0.89, the area per lipid outside is approx. 3 times that corresponding to the lipid inside.

The scheme depicted in Fig. 7, might illustrate the accommodation of the lipids with a higher area outside considering the interdigitation inferred from the methodologies employed.

In conclusion, arbutin stabilizes lysoPC molecules in aggregates larger than those formed by pure lysoPC. The particles observed can be modelized as vesicles in which part of the phosphates are facing an internal media by assuming an interdigitation of the acyl chain with arbutin molecules intercalated between them. The complex is stabilized by the formation of hydrogen bonds of arbutin with the phosphate and carbonyl groups and by hydrophobic interaction of the phenol groups with the terminal methyls. The model fits reasonably with the geometrical dimensions of the vesicles observed by electron microscopy.

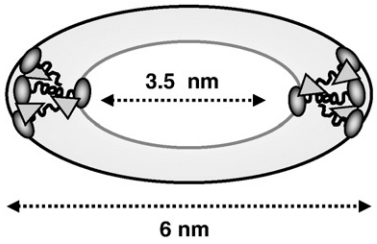

Fig. 7. Schematic representation of the lysoPC–arbutin vesicles showing the interdigitation and the inner and outer lipid ratio.

Acknowledgements

This work was supported with funds from Agencia Nacional de Promoción Científica y Tecnológica, Grant PICT 0324, CONICET (PIP 5476), and UBACyT 047.

PRL, AMG, and EAD are members of the Research Career of CONICET (Consejo Nacional de Investigaciones Científicas y Técnicas de la República Argentina).

References

[1] S.D. Brown, B.L. Baker, J.D. Bell, Quantification of the interaction of lysolecithin with phosphatidylcholine vesicles using bovine serum albumin: relevance to the activation of phospholipase A_2, Biochim. Biophys. Acta 1168 (1993) 13–22.

[2] B.L. Baker, B.C. Blaxall, D.A. Reese, G.R. Smith, J.D. Bell, Quantification of the interaction between lysolecithin and phospholipase A_2, Biochim. Biophys. Acta 1211 (1994) 289–300.

[3] M.A. Frías, S.B. Díaz, N.M. Ale, A. Ben Altabef, E. Disalvo, A FTIR analysis of the interaction of arbutin with dimyristoylphosphatidylcholine in anhydrous and hydrated states, Biochim. Biophys. Acta 1758 (2006) 1823–1829.

[4] M.A. Frías, A. Nicastro, N. Casado, A.M. Gennaro, S.B. Díaz, E.A. Disalvo, Arbutin blocks defects in the ripple phase of DMPC bilayers by changing carbonyl organization, Chem. Phys. Lipids 147 (2007) 22–29.

[5] Y. Tokiwa, M. Kitagawa, T. Raku, S. Yanagitani, K. Yoshino, Enzymatic synthesis of arbutin undecylenic acid ester and its inhibitory effect on melanin synthesis, Bioorg. Med. Chem. Lett. 17 (11) (2007) 3105–3108 (1).

[6] P.R. Cullis, B. de Kruijff, Lipid polymorphism and the functional roles of lipid in biological membranes, Biochim. Biophys. Acta 559 (1979) 399–420.

[7] N. Fuller, R.P. Rand, The influence of lysolipids on the spontaneous curvature and bending elasticity of phospholipid membranes, Biophys. J. 81 (2001) 243–254.

[8] F.C. Reman, R.A. Demel, J. De Gier, L.L.M. Van Deenen, H. Eibl, O. Westphal, Studies of the lysis of red cells and bimolecular lipid leaflets by synthetic lysolecithins, lecithins and structural analogs, Chem. Phys. Lipids 3 (1969) 221–233.

[9] G.A. Senisterra, E.A. Disalvo, J.J. Gagliardino, Osmotic dependence of the lysophosphatidylcholine lytic action on liposomes in the gel state, Biochim. Biophys. Acta 941 (1988) 264–270.

[10] E.A. Disalvo, L.I. Viera, L.S. Bakas, G.A. Senisterra, Lysophospholipids as natural molecular harpoons sensing defects at lipid interfaces, J. Coll. Interf. Sci. 178 (1996) 417–425.
[11] S.B. Díaz, A.C. Biondi de López, E.A. Disalvo, Dehydration of carbonyls and phosphates of phosphatidylcholines determines the lytic action of lysoderivates, Chem. Phys. Lipids 122 (2003) 153–157.
[12] L. Ramsammy, H. Brockerhoff, Lysophosphatidylcholine–cholesterol complex, J. Biol. Chem. 257 (1982) 3570–3574.
[13] M.J. Karnovsky, A formaldehyde–glutaraldehyde fixative of high osmolarity for use in electron microscopy, J. Cell Biol. 27 (1965) 137–338.
[14] M.P. Veiga, J.L. Arrondo, F.M. Goñi, A. Alonso, D. Marsh, Interaction of cholesterol with sphingomyelin in mixed membranes containing phosphatidylcholine, studied by spin-label ESR and IR spectroscopies. A possible stabilization of gel-phase sphingolipid domains by cholesterol, Biochemistry 40 (2001) 2614–2622.
[15] O.H. Griffith, P.C. Jost, Spin labels in biological membranes, in: L.J. Berliner (Ed.), Spin Labeling: Theory and Applications, Academic Press, New York, 1976, p. 454.
[16] R. Mendelsohn, H.H. Mantsch, in: A. Watts, A. DePont (Eds.), Progress in Protein–Lipid Interactions, Elsevier Science Publishers BV, Amsterdam, 1986, pp. 103–146.
[17] D. Marsh, L.I. Horváth, Spin label studies of the structure and dynamics of lipids and protein in membranes, in: Hoff (Ed.), Advanced EPR: Applications in Biology and Biochemistry, Elsevier, Amsterdam, 1989.
[18] S.B. Díaz, F. Amalfa, A.C. Biondi de López, E.A. Disalvo, Effect of water polarized at the carbonyl groups of phosphatidylcholines on the dipole potential of lipid bilayers, Langmuir 15 (15) (1999) 5179–5182.
[19] W. Hübner, A. Blume, Interactions at the lipid–water interface, Chem. Phys. Lipids 96 (1–2) (1998) 99–123.
[20] H.H. Mantsch, R.N. McElhaney, Phospholipids phase transitions in model and biological membranes as studied by infrared spectroscopy, Chem. Phys. Lipids 57 (1991) 213–226.
[21] I.C.P. Smith, Application of Solid State NMR to the lipids of model and biological membranes, in: J.W. Pettegrew (Ed.), En "NMR: Principles and Applications to Biomedical Research", Springer—Verlag, New York, 1990, p. 142.
[22] E.J. Dufourc, C. Mayer, J. Stohrer, G. Althoff, G. Kothe, Dynamics of phosphate head groups in biomembranes. A comprehensive analysis using phosphorus-31 nuclear magnetic resonance lineshape and relaxation time measurements, Biophys. J. 61 (1992) 42–57.
[23] R. Mendelsohn, C.R. Flach, Infrared reflection-absorption spectroscopy of lipid, peptides, and proteins in aqueous monolayers, in: S.A. Simon, T.J. McIntosh (Eds.), Current Topics in Membranes, vol. 52, Academic Press, San Diego, 2002, pp. 57–88.
[24] M.C. Luzardo, F. Amalfa, A. Núñez, S. Díaz, A.C. Biondi de López, E.A. Disalvo, Effect of trehalose and sucrose on the hydration and dipole potential of lipid bilayers, Biophys. J. 78 (2000) 2452–2458.
[25] A.E. Oliver, D.K. Hincha, N.M. Tsvetkova, L. Vigh, J.H. Crowe, The effect of arbutin on membrane integrity during drying is mediated by stabilization of the lamellar phase in the presence of nonbilayer-forming lipids, Chem. Phys. Lipids 111 (1) (2001) 37–57.
[26] P. Nambi, E.S. Rowe, T.J. McIntosh, Studies of the ethanol-induced interdigitated gel phase in phosphatidylcholines using the fluorophore 1, 6-diphenyl-1, 3, 5-hexatriene, Biochemistry 27 (1988) 9175–9182.
[27] P.R. Levstein, A.M. Gennaro, M.M. Pincelli, ^{31}P NMR and spin label EPR as complementary techniques for lipid polymorphism studies, in: Baruzzi Condat (Ed.), Recent Research Developments in Biophysical Chemistry, Research Signpost., India, 2002, pp. 165–180.